Trends in Cardiovascular Medicine 29 (2019) 83–94

Contents lists available at ScienceDirect

Trends in Cardiovascular Medicine

journal homepage: www.elsevier.com/locate/tcm

Cardiovascular magnetic resonance imaging for amyloidosis: The state-of-the-art ☆

Chun Xiang Tang[a], Steffen E. Petersen[b,c], Mihir M. Sanghvi[b], Guang Ming Lu[a], Long Jiang Zhang, PhD, MD[a,*]

[a] Department of Medical Imaging, Jinling Hospital, Medical School of Nanjing University, Nanjing, Jiangsu 210002, China
[b] William Harvey Research Institute, NIHR Biomedical Research Centre at Barts, Queen Mary University of London, Charterhouse Square, London EC1M 6BQ, UK
[c] Barts Heart Centre, Barts Health NHS Trust, West Smithfield, London, UK

ARTICLE INFO

Keywords:
Amyloidosis
Cardiac magnetic resonance imaging
Late gadolinium enhancement
T1 mapping
Extracellular volume

ABSTRACT

Amyloidosis results from insoluble precursor proteins being deposited in the extracellular compartment. The prognosis of the disease is predominantly determined by cardiac involvement due to amyloid accumulation that contributes to cardiac dysfunction and disturbed conduction of cardiac electrical signals. The clinical and radiological manifestations of amyloidosis are often non-specific, making amyloidosis a diagnostic challenge both for clinicians and radiologists. Cardiovascular magnetic resonance imaging, including conventional sequences, late gadolinium enhancement, T1 mapping and determination of extracellular volume fraction is a multi-dimensional modality for the assessment and diagnosis of cardiac amyloidosis and, in addition, is an excellent tool for risk stratification and disease tracking.

Introduction

The deposition of protein fibrils, which fold incorrectly in a β-pleated sheet, causes a group of rare diseases called systemic amyloidosis [1]. Cardiac amyloidosis (CA) is caused by accumulation of amyloid in the myocardial interstitium and associated with increased ventricular wall thickness and mass, which results in diastolic and, ultimately, systolic dysfunction. The majority of patients with CA have either immunoglobulin light-chain amyloidosis (AL) or transthyretin amyloidosis (ATTR), which may be hereditary, associated with transthyretin gene (mTTR) mutations, or wild-type (wtTTR). AL is the most common type of systemic amyloidosis and cardiac involvement is seen in more than half of patients [2,3], even up to 70% [4]. Cardiac ATTR is often a fatal condition that may be under diagnosed with 26% incidence and an underestimated cause of heart failure in specific ethnic populations and the elderly [5,6]. Specifically, mTTR amyloidosis is variable depending on the mutation [7], and wtTTR amyloidosis is probably much more common than is widely appreciated in elderly patients with heart failure with preserved ejection fraction [7]. The median overall survival of patients with CA is significantly shorter than that of patients without cardiac involvement [9], but survival is certainly improved with earlier diagnosis [8]. Diagnosis is challenging; however, early diagnosis and classification of CA are especially crucial given that the specific treatments hold great promise for improving survival in these fatal diseases [10,11].

The initial non-invasive test of choice to diagnose amyloid cardiomyopathy is echocardiography. Although infiltration of the myocardium by amyloid proteins shows increased echogenicity described as “sparkling”, it is not a sensitive finding for cardiac amyloidosis [12]. Nuclear scan is considered when echocardiography and CMR are not diagnostic but cardiac amyloidosis is still a suspicion in patients [13]. Cardiovascular magnetic resonance (CMR) is an important imaging modality due to its high specificity in the diagnosis of CA [9], is a powerful alternative to biopsy in the diagnosis of cardiac amyloidosis with sensitivity and specificity of 100% and 80% in establishing the diagnosis of cardiac involvement [14]. CMR should be considered for patients with unexplained heart failure and arrhythmias, especially when there is a suspicion of amyloid [15] and the echocardiogram is inconclusive with

Abbreviations: CA, cardiac amyloidosis; AL, immunoglobulin light-chain amyloidosis; ATTR, transthyretin amyloidosis; mTTR, transthyretin gene mutation; wtTTR, wild-type transthyretin gene; CMR, cardiac magnetic resonance imaging; ECV, extracellular volume; LGE, late gadolinium enhancement; PSIR, phase sensitive inversion recovery; PET/MR, positron emission tomography/magnetic resonance imaging; SPECT, single-photon emission computed tomography; EF, ejection fraction; cTnT, cardiac troponin T; NT-proBNP, N-terminal pro–B-type natriuretic peptide; DTI, diffusion tensor imaging.

☆ Declarations: Ethics approval and consent to participate. Not applicable.

* Corresponding author.
E-mail addresses: 522956587@qq.com (C.X. Tang), s.e.petersen@qmul.ac.uk (S.E. Petersen), m.sanghvi@qmul.ac.uk (M.M. Sanghvi), cjr.luguangming@vip.163.com (G.M. Lu), kevinzhlj@nju.edu.cn (L.J. Zhang).

https://doi.org/10.1016/j.tcm.2018.06.011
1050-1738/

the disease [16] . Thus, CMR has been considered as imaging reference for cardiomyopathy [17]. CMR can perform myocardial tissue characterization in addition to conventional volume and function evaluation. CMR with T1 mapping is sensitive to amyloid deposition and myocyte response to infiltration making it an attractive tool for non-invasive monitoring of disease progression. With intravenous administration of gadolinium contrast medium, late gadolinium enhancement imaging and determination of extracellular volume fraction (ECV) add additional useful diagnostic and prognostic information. Our objectives for this article are to: 1) review CMR imaging of amyloidosis in biomedical research and clinical practice, and 2) briefly outline future challenges and opportunities of CA in CMR.

CMR techniques

Conventional sequences

Over the years, CMR has emerged as the reference standard for the evaluation of ventricular morphology and function. Cardiac cine MR can provide accurate imaging of myocardial mass, atrial/ventricular structure, as well as atrial and ventricular function and of typical morphological features of restrictive cardiomyopathy with preserved ejection fraction. In contrast to EF, stoke volume has a high probability of being abnormal in the earlier stages of cardiac amyloid infiltration. This could be due to the initial increase in myocardial mass conferring a smaller end-diastolic cavity volume [18]. CMR is conventionally limited in evaluating cardiac diastolic function [19]. But strain, strain rate, and torsion can be extracted from CMR data with tagging, feature tracking and velocity coding MR techniques, which provide new dimensions to evaluate diastolic function. Another CMR-specific way to assess diastolic function is based on the concept of “T1 mapping” [20]. All these techniques provide indirect ways to cardiac diastolic function evaluation. Since 2010, several MRI-conditional and non-conditional cardiac implanted electronic devices have been developed and approved for use with multiple MRI imaging modalities [21–25]. Whereas two decades ago cardiac implanted electronic devices were viewed as absolute contraindications to perform MR [26], many MRI studies are now being performed safely using published protocols [27,28]. However, in most centers, cardiac implanted electronic devices are still considered contraindications to MRI. A primary advantage of CMR is the unique ability to analyze tissue composition with “myocardial tissue characterization” [29]. The signal detected with non-contrast T1, T2 from the myocardium can be used to differentiate the normal from abnormal myocardium but with limited value. Previous reports have not described any presence of edema in CA, reflected by no T2 signal changes being observed [19,30]. However, whether high native myocardial T1 correlates with troponin release or high T2 remains unclear as outlined by Fontana et al. [31]. It is generally accepted that the most common types of CA: AL and ATTR, overlap in respect to their CMR manifestations [32,33].

Late gadolinium enhancement (LGE) technique

LGE works on the basis of the difference in contrast agent washout between normal and abnormal myocardium. This gadolinium contrast agent is small enough to accumulate in the extracellular space but not so small so as to cross intact cellular membranes [34]. Gadolinium contrast agent reduces the T1 relaxation time of tissue. In areas of “scar” tissue, or in regions of amyloid deposition, the impermeability of gadolinium contrast agent is prolonged compared with normal myocardium. After administration of gadolinium contrast agent in healthy tissue, diffuse lowering of T1 in the whole myocardium will happen. In focal amyloid/scar area regional T1 values are detectably lower, which forms the basis of LGE for qualitative detection [19]. A global subendocardial LGE pattern, the most typical LGE pattern in CA, demonstrates subendocardial arc shaped or annular high signal in a non-coronary artery territory area, but transmural or patchy LGE with diffuse or localized amyloid infiltration enrich the patterns [32,35] (Fig. 1). LGE findings in CA are not dichotomous but a continuum from no LGE to subendocardial, to transmural tracking with increasing amyloid deposition. LGE can be obtained through a cumbersome primed contrast infusion or bolus administration of gadolinium contrast agent, the former is hard to be carried out and not used widely, and the latter can be performed 10 min, or 15–20 min delay after bolus administration [36–38]. However, adequate differentiation between normal and abnormal myocardium on contrast–enhanced MR images has been shown 5–8 min after gadolinium administration instead of the imaging delay of 10–20 min generally used in contrast-enhanced cardiac MR imaging [39]. Inversion times to null the myocardium are variable and difficult to set, especially in CA, because accelerated clearance of gadolinium contrast agent occurs when it encounters beta-pleated sheets and protein fibrils causing CA.

Limitations and drawbacks of LGE have to be mentioned. Firstly, adverse reactions following intravenous administration of gadolinium based contrast agents are rare but may be potentially fatal, including anaphylaxis and nephrotoxicity, especially when given at high doses (>0.3 mmol/kg) or in patients with renal dysfunction [40,41]. Besides adverse reactions, it can be challenging to identify the diffuse cardiac amyloidosis due to diffuse late gadolinium enhancement when conventional LGE techniques are employed. Furthermore, standard LGE imaging techniques are flawed in amyloidosis as there is a requirement that the MR technologist/radiographer selects the inversion time to optimally null signal from regions of normal myocardium. Amyloidosis that involves the whole myocardium may have no normal myocardium, resulting in “wrong” LGE patterns or false negative findings (global myocardium involved but could appear as normal) [19]; these issues can be ameliorated with phase sensitive inversion recovery (PSIR) sequences, or LGE combined with T1 mapping mentioned below. Unclear borders between abnormal enhanced myocardium and blood on bright-blood PSIR sequence would affect the accuracy of LGE and transmurality measurements, black-blood PSIR LGE has been introduced to improve the contrast between the blood pool and abnormal myocardium by exploiting an inversion pulse in combination with a T2 preparation module [42,43], with 2D acquisitions that are performed during a breath-hold [44] or a 3D free-breathing whole-heart acquisitions [45].

T1 mapping

T1 mapping is the quantitative measurement of myocardial signal, and can be performed pre-contrast (native T1) and post-contrast. Each pixel of the image reflects the absolute value of T1, coded in color, therefore, myocardial native T1 mapping measures intrinsic myocardial signal (Fig. 2). Benefits of native T1 mapping without the administration of contrast agent would be the independence of the outcome of the quantitative T1 map from renal function and the timing of the measurement [46]. The reference value of native T1 depends on the strength of the magnetic field and the scanner and sequence used (Table 1) [38,47–60]. Pathological status will change native T1 of the myocardium. Reduced T1 occurs uncommonly in fat infiltration, i.e. Fabry disease and iron overload [58,61]. Increased native T1 values commonly occur in diffuse myocardial fibrosis, scar, amyloidosis and edema. This may have clinical value particularly when gadolinium-based contrast agents are contraindicated. In both amyloidosis types, T1 mapping can track the changes of myocardium earlier than systolic and

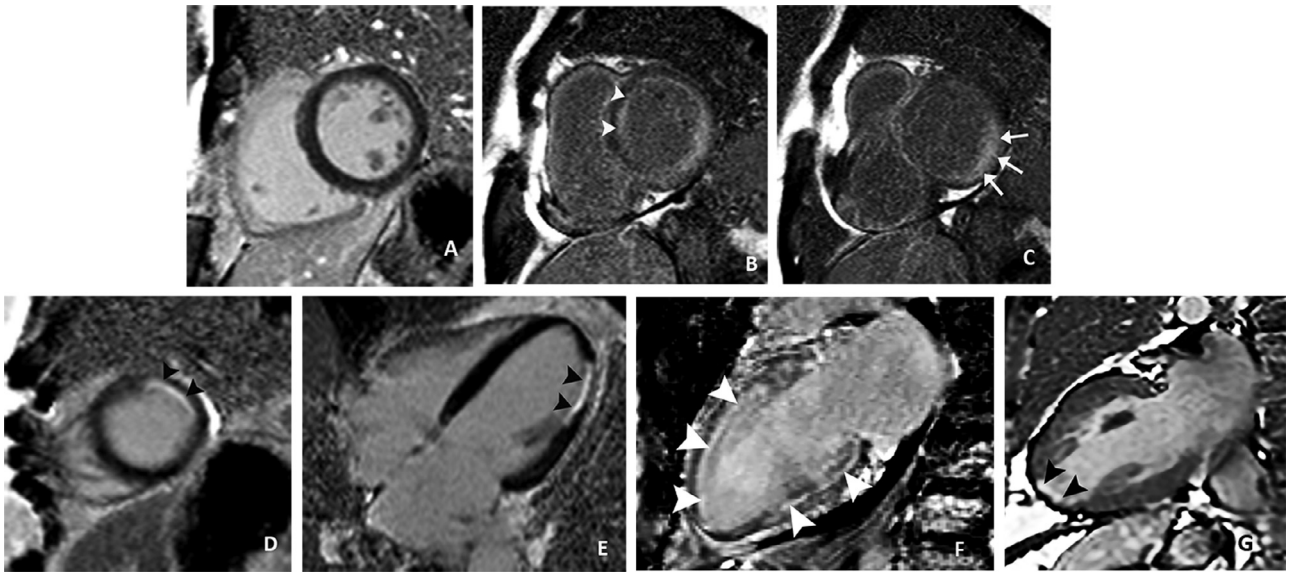

Fig. 1. Different LGE patterns in patients with cardiac amyloidosis.
Images shown include short-axis and four-chamber views of late gadolinium enhancement (LGE) with phase-sensitive inversion recovery reconstruction (PSIR) in a 40-year-old female healthy volunteer (panel A), a 53-year-old male patient (panels B, C) with AL amyloidosis; a 76-year-old female patient (panels D, E) with myocardial infarction. The image of the healthy volunteer (panel A) show no LGE; subendocardial LGE is shown in a patient with AL amyloidosis (white arrowheads in panel B), while transmural LGE is seen in a same patient (white arrows in panels B and C). LGE in cardiac amyloidosis can be distinguished from myocardial infarction, which typically corresponds with a coronary artery territory as in this patient with circumflex branch of left coronary artery as the infarct culprit artery in panels D and E (black arrowheads). Two-chamber view of a 56-year-old male patient (panel F) shows the thinning of left ventricle region wall resulting from myocardium infarction presenting with striped sharp-marginal LGE, compared with diffuse vague-marginal subendocardial LGE in a 46-year-old male patient (arrowheads on panel G).

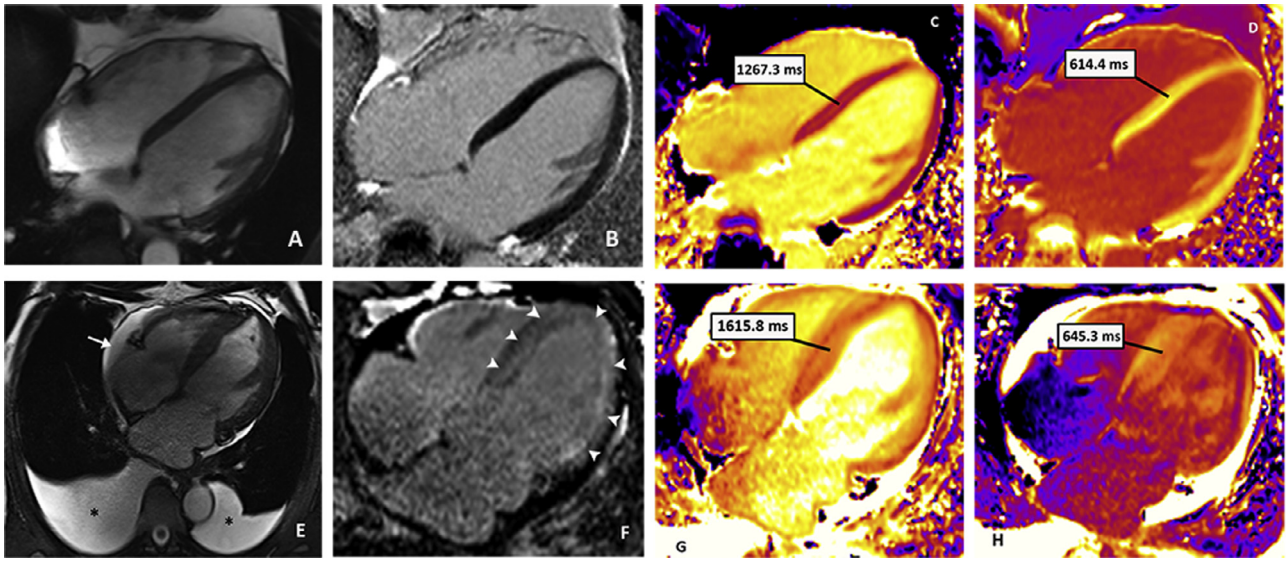

Fig. 2. Comprehensive comparison with cardiac MR between a patient with AL cardiac amyloidosis and a healthy volunteer.
Images shown include four-chamber view cine (panels A, E), corresponding late gadolinium enhancement (LGE) image with phase-sensitive reconstruction (panels B, F), native T1 maps, (panels C, G) and post-contrast T1 maps (panels D, H) in a 38-year-old male healthy volunteer (top row) and a 57 -year-old male patient with AL amyloidosis (bottom row). The healthy volunteer has normal cine, LGE images and native T1 value, with normal calculated extracellular volume (ECV) of 0.253, while the AL amyloidosis patient after 3 months of autologous stem cell transplantation has pericardial effusion (white arrow in panel E), bilateral pleural effusion (* in panel E); transmural LGE (white arrowheads in panel F) with very high native T1 values and high ECV values (0.439) are seen.

Table 1
Normal Native T1 and ECV values reported using different pulse sequences at 1.5 and 3 T.

	Native T1 (ms)		ECV (%)	
Sequence	1.5T	3T	1.5T	3T
17-HB MOLLI (41)	986 ± 45 (51)	1070 ± 55 (56)	23 ± 3 (60)	27 ± 9 (56)
ShMOLLI11 (42)	958 ± 20 (52, 53)	1178 ± 13 (57)	27 ± 2 (43)	Not reported
SASHA14 (43)	1177 ± 27 (54)	1539 ± 50 (58)	22 ± 3 (54)	21.3 ± 2 (49)
SAPPHIRE15 (44)	1212 ± 40 (55)	1578 ± 35 (59)	20 (38)	20.2 ± 2 (49)

HB indicates heart beat; SASHA, saturation recovery single-shot acquisition. SAPPHIRE, saturation pulse-prepared heart rate–independent inversion recovery.
The number in parentheses is reference order number.

diastolic function, myocardium mass and can be used as a prognostic marker [5,52].

The main drawbacks of T1 mapping techniques are: firstly, it measures mixed myocardial signal of both interstitium and myocytes. Secondly, the T1 values in the T1 map are variable according to the pulse sequence and magnetic resonance scanner, and use of native T1 mapping for diagnosing diffuse CA might be challenging. On PSIR, perfect concordance between myocardial T1 value and LGE has been reported, that is, areas of low T1, coded with the darkest blue, represent areas of LGE. As mentioned before, it is difficult to interpret diffuse LGE when no normal myocardium exists using traditional LGE sequences. When the entire myocardial native T1 value is lower than blood pool, global LGE exists; global LGE is also present if it is seen on LGE images with PSIR or if the myocardium nulled before the blood pool on a cine multiple inversion time sequence because the chelation of amyloid beta-pleated sheet protein and gadolinium contrast agent can accelerate the washout of the gadolinium contrast agent, which make it unique in CA [62,63]. Thirdly, normal T1 values are higher when measured at 3.0 T scanner or with different/new sequences [55,64].

It is not easy to quantify and interpret diffuse LGE and this is why the emergence of the extracellular volume (ECV) technique has been invaluable. Technically, calculation of ECV should require the equilibration of contrast concentrations between myocardium and blood pool. Gadolinium contrast agent allows another method to analyze tissue characterization with T1 mapping. Post-contrast T1 value may be lower in some cardiac conditions, suggesting increased myocardial interstitial space, but change with the time of delay after administration of the gadolinium contrast agent, which limits its evaluation of myocardium separately. With the pre- and post-contrast T1 of myocardium and blood, adjusted for hematocrit, ECV can be calculated, using the following formula:

$$\mathrm{ECV} = (1 - \mathrm{hematocrit})\left(\Delta \mathrm{R1}_{\mathrm{myocardium}} / \Delta \mathrm{R1}_{\mathrm{blood\ pool}}\right) \quad (1)$$

where $\Delta \mathrm{R1}_{\mathrm{myocardium}}$ or $\Delta \mathrm{R1}_{\mathrm{blood\ pool}}$ indicates change in blood and myocardium pre- and post-Gd and $\mathrm{R1} = 1/\mathrm{T1}$ [47]. Reference range of ECV is shown in Table 1 [46–60].

Disadvantages of ECV are as follow: an ECV calculation requires two different T1 maps, one before and one after contrast agent injection, which needs more imaging time. Furthermore, as the hematocrit value is acquired by a blood sample that needs to be taken and analyzed in order to obtain the hematocrit, which produces a time-consuming procedure in a busy clinical workflow. The resulting ECV map, representing the volume distribution of extracellular tissue components [65] (Fig. 2), can only be calculated combined with pre-, post-T1 map, and the hematocrit value. Further attempts to overcome these problems and simplify the procedure would be welcomed.

New MR techniques

All above mentioned techniques show clinical value in CA, nonetheless, limitations of these techniques still exist, which stimulates the search for other new imaging modalities, i.e. positron emission tomography/magnetic resonance imaging (PET/MR), myocardial deformation imaging and CMR elastography. It is worthwhile mentioning that CMR cannot definitively distinguish AL from ATTR, while single-photon emission computed tomography (SPECT) using bone tracers ^{99}mTc-3,3-diphosphono-1,2-propanodicarboxylic acid, ^{99}mTc-Hydroxymethylene diphosphonate, ^{99}mTc-pyrophosphate has been reported to differentiate the two types of amyloidosis [66]. PET/MR is essentially fused PET and MR LGE imaging, in which PET activity can be detected and quantified within the specific areas of amyloid deposition visualized on LGE. PET/MR with ^{18}F-sodium fluoride has shown the potential to diagnose CA, identify characteristic LGE, assess cardiac function, and differentiate AL from ATTR within a single scan in a clinical study with a small sample [67], so further research with a larger sample size needs to be done in future. According to Trivieri et al.'s study [67], MR LGE images that allowed PET activity to be measured within the myocardium and specific areas of amyloid deposition visualized on LGE are best suited for the application PET/MR. Considering a good correlation between the burden of amyloid on native T1 mapping and ^{18}F-sodium fluoride PET uptake was observed, T1 mapping is a subsequent best suited sequence next to LGE.

The analysis of myocardial strain offers new insight into the disease's mechanisms using heart deformation analysis and feature tracking including displacement, velocity, strain, and strain rates, providing a new dimension to investigate CA. Echocardiography, the initial non-invasive test of choice to diagnose CA, is diagnostic of CA with "granular sparkling" or "speckling" of the infiltration by amyloid proteins in myocardium [13]. Various deformation metrics derived from echocardiography could help differentiate cardiac amyloidosis from other causes of LV thickening [68–70], or predict the survival [71] or identify early cardiac improvement following treatment for AL amyloidosis [72]. It is validated that differences exist in myocardial function and motion patterns between patients with CA and healthy subjects by measuring segmental myocardial motion indexes on cardiac cine images [73]. Overall, global longitudinal strain was decreased in amyloid heart disease and was reported to have predicted reduced survival [74]. However, global longitudinal strain in CA has a typical pattern with reduced strain at the left ventricular base and progressively increased strain near the left ventricular apex (Fig. 3). Left ventricle twisting and untwisting motions are initially increased in patients with AL with no cardiac involvement, but they may normalize or become reduced with progressive cardiac involvement [75]. Recently, Oda et al. [76] measured the left ventricular global circumferential strain of LGE-positive and LGE-negative patients with systemic amyloidosis using CMR tagging. As a result, the sensitivity, specificity, and accuracy with circumferential strain parameters for the identification of LGE-positive amyloidosis were 93.8%, 76.9%, and 90.2%, respectively, and the peak circumferential strain and variability in the peak circumferential strain time may correlate with the severity of cardiac amyloid infiltration and may be more sensitive than LGE for the identification of early cardiac involvement in patients with amyloidosis.

Last, shear wave elastography techniques relying on an external vibrating source can produce shear waves inside a tissue of interest. MR elastography, based on the new approaches, can measure the vibrational displacements in the tissue. The displacement field is used to form a stiffness map through the inversion from one mathematical algorithm. This technique has been applied in CA. CMR elastography was performed to measure left ventricular stiffness, demonstrating that the myocardial stiffness of CA patients was significantly higher than normal controls in recent works [77,78].

The advantages and disadvantages of above-mentioned CMR techniques used in CA are summarized in Table 2.

CA diagnosis

Cardiac function

Cardiac amyloid deposition can cause low end diastolic volume, poor filling, thus poor diastolic relaxation and finally systolic dysfunction [6]. Conventional indicators like ejection fraction (EF) may be normal even in the late phase of CA because it is poor to assess systolic function in patients with concentric remodeling, while stroke volume, the indexed stroke volume, cardiac output, usually markedly reduced, are therefore better markers of systolic function

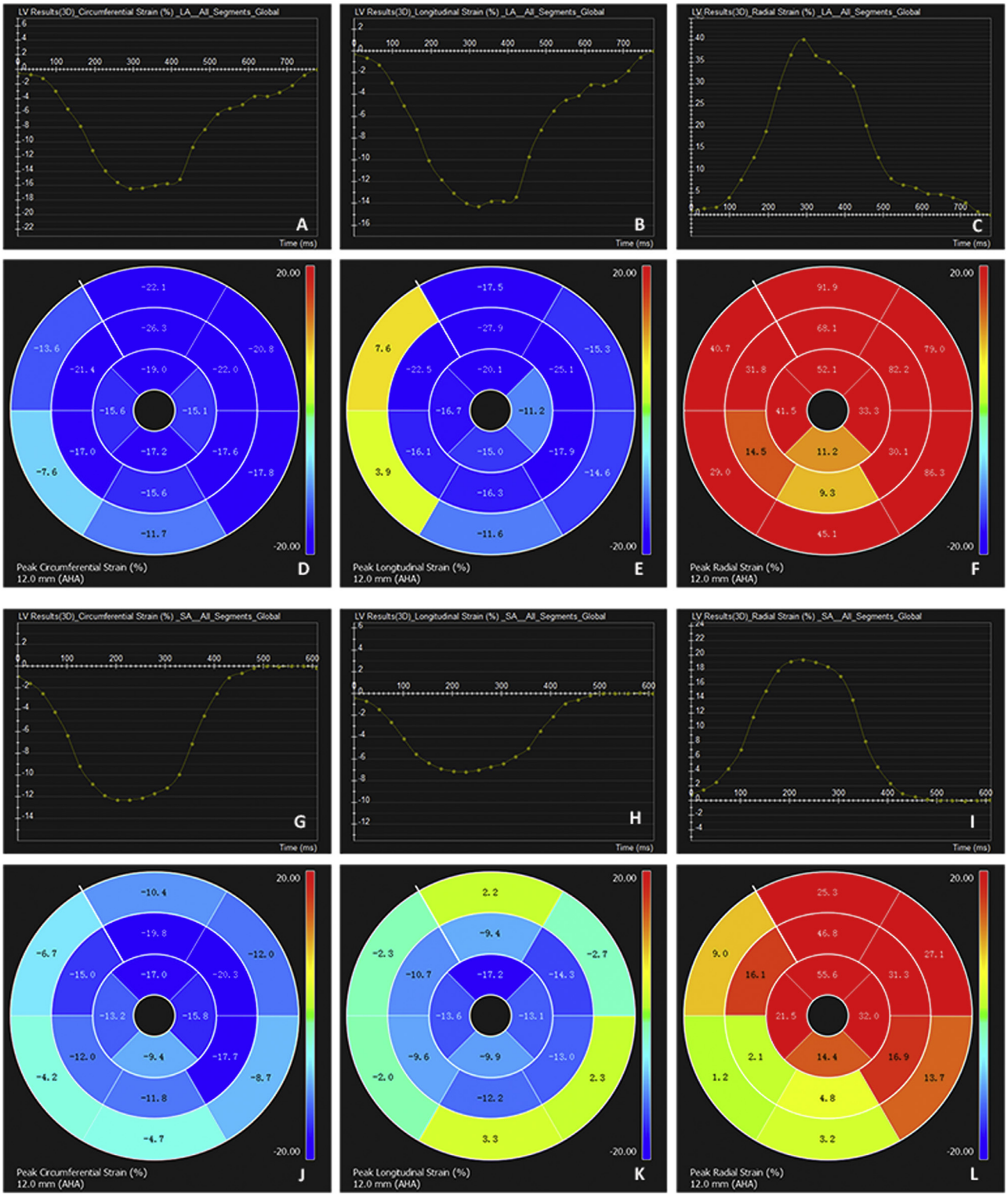

Fig. 3. Strain curves and polar maps in two patients with AL amyloidosis based on 3.0 T cardiac cine MR.
Strain curves (panels A–C, G–I) and polar maps (panels D–F, J–L). Panels A–F: 45 -year-old female patient has a native T1 value of 1307.5 ms and ECV of 0.317 but no late gadolinium enhancement on cardiac MR. Global circumferential strain (GCS) and (global longitudinal strain) GLS are decreased in the basal inferior and lateral wall of the left ventricle. Panels G–L: 61 -year-old male patient with cardiac amyloidosis has a native T1 value of 1546.2 ms and ECV of 0.652, characterized with diffuse transmural late gadolinium enhancement in cardiac MR. GCS, GLS and global radial strain (GRS) are all decreased in this patient with cardiac amyloidosis and have a characteristic pattern with reduced strain (green and light blue) at the LV base and progressively increased strain near the LV apex.
ECV = extracellular volume; GCS = global circumferential strain; GLS = global longitudinal strain; GRS = global radial strain.

Table 2
The advantages and disadvantages of CMR techniques used in cardiac amyloidosis.

CMR techniques		Advantages	Disadvantages
Conventional sequences (T1, T2, cine)		Intrinsic signal without contrast agent	1. Limited value in diastolic function 2. Unresolved correlation between high native myocardial T1 and high T2
LGE		1. Robust evidence to detect CA	1. Adverse reactions and nephrotoxicity of gadolinium contrast agents, but rare
		2. More specific and sensitive than CMR functional assessment	2. Relatively operator-dependent setting of inversion time 3. Not easy to quantify and interpret diffuse LGE
T1 mapping	Native T1 mapping	1. Without the use of contrast agents	1. Mixed myocardial signal from both interstitium and myocytes
		2. Quantitative value for diagnosis, prognosis as well as follow up	2. Sensitive to the pulse sequence and scanner used 3. Difficulty in differentiating edema and amyloid unambiguously
	ECV	1. Earlier disease marker than LGE and T1 value	1. Prolonged exam time with acquisition of two different T1 maps
		2. More robust and specific in CA with ECV > 0.4	2. An additional time-consuming procedure requiring the drawing of blood for the hematocrit value
		3. Quantitative index for diagnosis, prognosis as well as follow up	3. Contrast is required and thereby same potential rare reaction and nephrotoxicity
PET/MR		To quantify myocardial activity, in vivo show amyloidosis and establish diagnosis of CA within a single scan	1. Associated with radiation exposure
Myocardial deformation imaging		To provide information on regional wall motion abnormalities and measure the degree of deformation of a myocardial segment	1. Through-plane motion artifacts 2. Limited by pixel size 3. No standardization 4. Clinical implications of this data is unknown and that remains research tool
CMR elastography		1. Without the use of contrast agents 2. To quantify myocardial stiffness	1. Not tolerated in all patients 2. Poor stiffness maps from respiratory motion, poor cardiac gating, inadequate wave penetration, and poor signal noise ratio 3. Clinical implications of this data is unknown and that remains research tool

CMR: cardiac magnetic resonance imaging; LGE: late gadolinium enhancement; CA: cardiac amyloidosis; ECV: extracellular volume.

than EF [29]. Long axis function in CA is characteristically reduced for both right ventricle and left ventricle disproportionately to apparent radial function. Apical function is preserved until late, commonly called “apical sparing”. The atria may be dilated, but a pure restrictive cardiomyopathy has more impressive atrial dilatation. CA should be suspected in any patients presenting with preserved ejection fraction and heart failure. If the EF is reduced in AL, then (unless already treated), patients are typically in heart failure with pleural and/or pericardial effusions, whereas ATTR appears to be better tolerated or more indolent in its progression. Still, a reduced left ventricular EF of 40% echocardiographically was reported in one recent work in 8% of patients with mTTR amyloidosis [79], and the mTTR patients also had decreased average left ventricular EF (47% with left ventricular EF < 40%) more frequently than patients without mTTR [80].

CMR has now become the gold standard in the assessment of the morphology and function of the heart, but cardiac function evaluation alone cannot prove the diagnosis of CA, since changes in morphology and function occur late. However, the information it provides can add to clinician confidence in making a diagnosis of CA. Further study on left ventricular regional myocardial microvascular function in AL patients showed significantly reduced first-pass perfusion upslope and maximal signal intensity, and increased time to maximum signal intensity compared with healthy control subjects [81]. Evaluation of myocardial microvascular function can also differentiate AL patients with preserved or impaired systolic function from healthy subjects [81]. Feature tracking CMR as well as first-pass perfusion imaging were recently successfully applied to monitor abnormal left ventricular myocardial deformation of AL patients with preserved left ventricular EF, and found myocardial deformation was associated with microvascular dysfunction [82].

Myocardial hypertrophy

Extracellular deposition of amyloid protein leads to this increase in wall thickness, and contributes to ventricular stiffening [83]. CA can present with asymmetric or symmetric, eccentric or concentric wall hypertrophy, thus increasing left ventricular mass (Fig. 4). Asymmetrical septal hypertrophy is defined as a ratio between the septal and posterior wall thickness >1.5, which is classically associated with hypertrophic cardiomyopathy. Worthy to be mentioned, the potential asymmetric septal hypertrophy pattern of cardiac amyloidosis can be confused for hypertrophic cardiomyopathy, but with LGE images the phenotypes are readily differentiated, which is key in differentiation of hypertrophic cardiomyopathy from amyloidosis if this pattern occurs. Such a phenotype is more common in ATTR [84] than AL and is common with the morphological subtypes of sigmoid septum and reverse septal contour. 5% of patients diagnosed with hypertrophic cardiomyopathy have cardiac mTTR [79]. Therefore, its presence should be used with caution to favor hypertrophic cardiomyopathy strongly over amyloidosis [8]. Besides, no difference was found in the prevalence of the different morphological phenotypes in wtTTR and mTTR CA. Right ventricular involvement with hypertrophy is also frequent [85]. Generally, myocardial hypertrophy in CA is defined as mean left ventricular wall or ventricular septum thickness >12 mm measured in the end-diastolic phase without hypertension or any other possible causes of left ventricular hypertrophy [86]. However, with the use of 12 mm as the cutoff for left ventricular wall thickness,

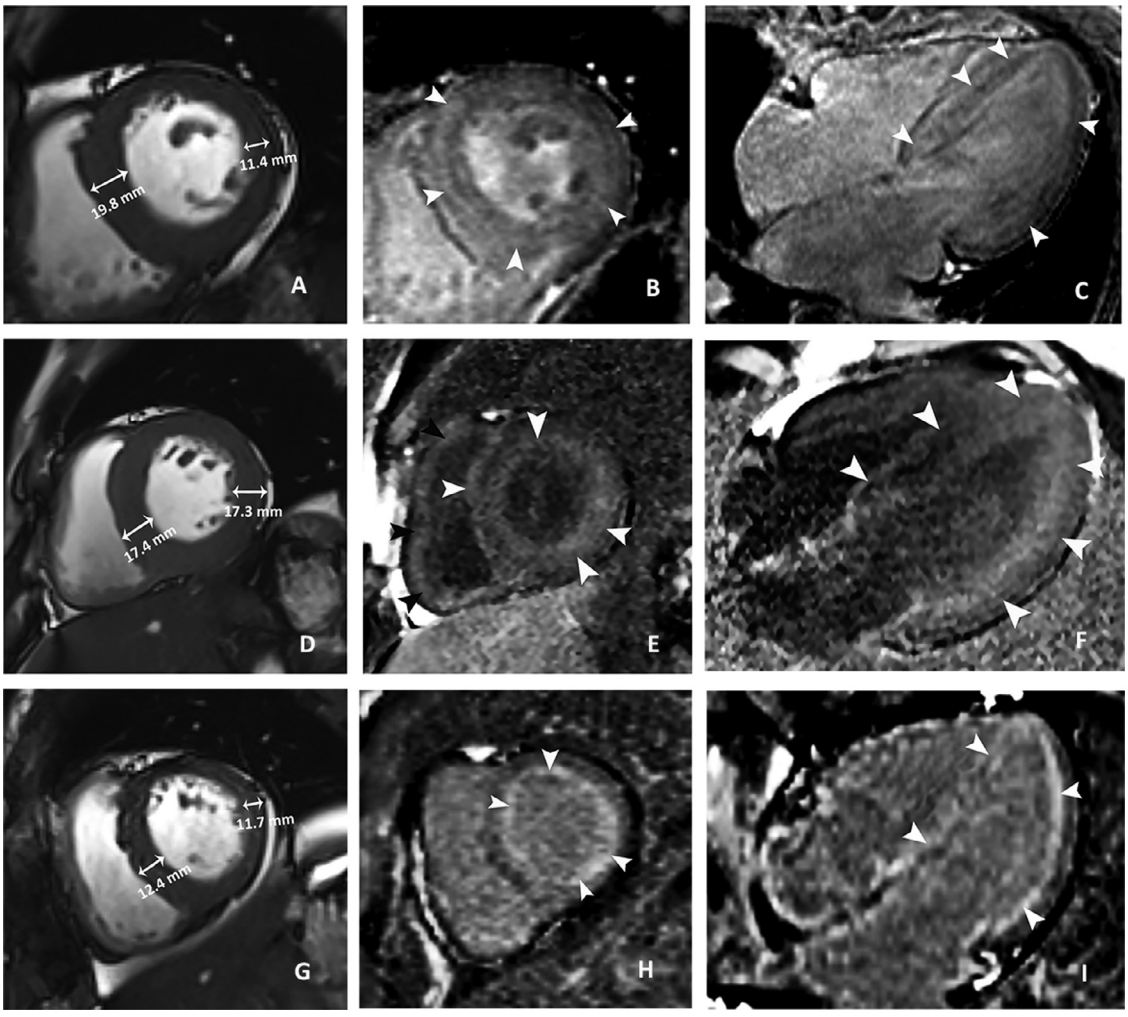

Fig. 4. Different myocardial hypertrophy patterns in amyloidosis.
Panels A-C show asymmetric and eccentric wall hypertrophy of cardiac amyloidosis in a 52-year-old woman on short-axis view cine image (panel A), short-axis view (panel B) and 4-chamber views with late gadolinium enhancement (LGE) imaging (panel C), while panel D displays symmetric and concentric wall hypertrophy on short-axis view cine image in a 54-year-old man, with white arrowheads pointing to transmural LGE of left ventricle (panel E) and black arrowheads of right ventricle (panel F). No wall hypertrophy is seen on short-axis view cine image (panel G) in a 55-year-old man, but obvious subendocardial LGE and local transmural LGE (arrowheads) are identified on short-axis and 4-chamber views with LGE imaging (panel H and I).

early CA may also remain undiagnosed. Recently, diastolic left ventricular posterior thickness >13 mm was regarded as the diagnostic criterion for CA, hypertrophic cardiomyopathy and unspecific cardiomyopathy [87]. However, no guideline is currently available to provide the consensus for diagnostic thresholds, thus more studies to validate such thresholds in both AL and ATTR are needed.

Myocardial tissue characterization

LGE of the left ventricular myocardium was long deemed to be the standard reference to detect cardiac amyloid deposition. In systematic amyloidosis, sensitivity and negative predictive value of 100% to diagnose CA with LGE have been reported, with specificity and positive predictive value of 80% and 81%, respectively [12]. Atrial wall and right ventricular free wall could be involved, which is rarely seen in ischemic heart disease [1]. More than 33% of left atrial LGE produced the greatest diagnostic value for CA, and the extent of left atrial LGE was highly predictive for CA diagnosis [88]. In ATTR, positive LGE was detected in 60% of mTTR patients [89]. And there was more extensive LGE with right ventricular involvement in individuals with ATTR than in those with AL [31]. Some attempts were made to distinguish AL from ATTR in patients with CA using CMR. Combining LGE score (The Query Amyloid Late Enhancement, QALE score) with wall thickness and age, ATTR presented with higher sensitivity of 87% and specificity of 96% compared with AL. Furthermore, 90% of patients with ATTR presented with transmural LGE, compared with 37% of patients with AL. The prevalence of transmural LGE and right ventricular LGE was significantly higher in ATTR than AL [31], which was consistent with another study that displayed there was no difference in LGE prevalence between wtTTR and mTTR [84].

Native T1 is a sensitive and early disease marker, increased before abnormality in blood biomarkers, left ventricle hypertrophy or presence of LGE [29]. Native T1 values are higher in diseases resulting in an elevation in the extracellular matrix compared to healthy subjects, which has been stated in myocardial edema [90], fibrosis [56] and amyloidosis [51]. Myocardial native T1 mapping may have a high diagnostic accuracy in both AL and ATTR compared with hypertrophic cardiomyopathy, a clinically relevant differential diagnosis [51]. Moreover, native myocardial T1 mapping can detect ATTR amyloidosis with similar diagnostic utility and disease tracking with AL amyloidosis, but with lower maximal T1 elevation, appearing to be an earlier disease marker in gene mutation carriers than LGE imaging [5].

Table 3
Differential diagnosis on AL and ATTR amylosidosis.

Indicators				Cardiac AL	Cardiac ATTR
Age (years)				62–65 (31, 32, 37, 41, 64)	69–73 (31, 32, 84)
Sex predilection				Not reported	Male (31, 32, 84)
Survival (months)				15.7–18 (32, 113)	38.9–45 (32, 113)
CMR	Morphology	Symmetrical LVH		68% (2, 84)	18% (84)
		Asymmetrical LVH		14% (2, 84)	79% (84)
		No LVH		18% (2, 84)	3% (84)
	Function	LVEDV (ml)		114–123 (32, 41, 84)	131 (32, 84)
		LVESV (ml)		19–43 (32, 37, 84)	32–59 (32, 84)
		LVEF (%)		59–66 (32, 37, 41, 84)	56 (32, 54)
		LV mass (g)		140–197 (32, 41, 84)	228–244 (31, 84)
		LA area (cm^2)		23–26 (32, 84)	26–31 (32,84)
		SV (ml)		70–71 (32, 84)	71–72 (32, 84)
	Tissue characterization	LGE	Subendocardial LGE	39% (63)	24%–29% (63, 84)
			Transmural LGE	27%–50% (63, 84)	63%–71% (63, 84)
			RV LGE	72%–77% (32, 84)	96%–100% (32, 84)
		T1 mapping (ms)		1080–1140 (31[a], 37[a], 52[a])	1101 –1097 (5[a], 31[a])
		ECV		0.53–0.54 (31, 84)	0.58–0.59 (31, 84)
	Pericardial effusion			37% (32)	33% (32)
	Pleural effusion			57% (32)	41% (32)

AL: light chain amyloidosis; ATTR: transthyretin amyloidosis; CMR: cardiac magnetic resonance imaging; LVH: left ventricular hypertrophy; LVEDV: left ventricular enddiastolic volume; LVESV: left ventricular end-systolic volume; LVEF: left ventricular ejection fraction; LV: left ventricular LA: left atrial; SV: stroke volume RV: right ventricular; LGE: late gadolinium enhancement; ECV: extracellular volume.
The number in parentheses is reference order number.
[a] Indicates the data measured with 1.5 T MR scanner.

It is worth mentioning that the lower native T1 value in ATTR patients than AL amyloidosis may result from a lower amyloid burden, less collagen or hydration due to amyloid, or differential effects on the intracellular signal, which was suggested in Fontana's later study [30]. Additionally, in AL, native T1 value correlates with reductions in limb lead voltages, whereas in ATTR, it associates with electrocardiogram PR and QRS duration and indexed left atrial area, a reduction in 6-min walk test [91]. Native T1 mapping also showed the potential value for the detection and quantification of cardiac involvement in familial amyloid polyneuropathy, induced by deposits of amyloid fibrils in nerves, the most commonly due to mTTR [92].

The diagnostic value of ECV is reflected in three parts: firstly, ECV in amyloidosis tends to be higher than in any other cardiomyopathies, ECV evaluation seems to provide a unique biomarker in this patient group [93–95]. Secondly, ECV was found to be elevated in patients who presented no cardiac involvement with LGE assessment and conventional testing, suggesting a potential value to detect CA earlier [95–97]. Thirdly, native T1 values are higher in AL than in ATTR, whereas the ECV is higher in ATTR than in AL [31], pointing to an extra process that may contribute in AL amyloidosis to the elevation of native T1, the most favored cause would be myocardial edema in AL [97]. ECV is more robust compared to native T1 values and LGE, especially across different centers as it is a ratio of T1 change. Moreover, high global ECV has high specificity in amyloidosis: fibrosis cannot result in an ECV of greater than 0,4 in remote (non-infarct) myocardium, suggesting that ECV $>$ 0.4 in remote myocardium becomes very specific, only with the need to differentiate from diffuse myocardial edema [29]. In addition, ECV was significantly different in mTTR compared with wtTTR amyloidosis. In patients with different mutations of ATTR amyloidosis, patients with V30M had a significantly lower ECV than patients with wtTTR, T60A, and V122I, and patients with V122I had significantly higher ECV than patients with T60A [84]. The key points for differential diagnosis of the two CA subtypes in CMR are shown in Table 3.

Risk stratification/ prognosis evaluation

Cardiac biomarkers are non-specific indicators of cardiac dysfunction, however, they tightly correlate with prognosis and therapeutic response in AL amyloidosis [98]. Current Mayo staging systems for CA are based on serum levels of NT-proBNP, cardiac troponin T (cTnT) and the concentration of circulating amyloidogenic free light chains (FLC) [99,100]. This staging system assigns patients a score of 1 for each differential free light chain (dFLC) $\geq$18 mg/dL, cTnT $\geq$0.025 ng/mL, and NT-proBNP $\geq$1800 pg/mL, creating stages I (no points) to IV (three points). These cardiac biomarkers are globally accepted as prognostic tools in amyloidosis [101]. In recent years, high sensitivity cardiac troponin T has set a novel gold-standard of generations assays, also providing prognostic value, particularly in AL amyloidosis [102]. Uric acid was also included in the risk staging system in a recent study [103].

Apart from laboratory measurements, ejection fraction, pericardial effusion [104], right ventricular systolic pressure, right ventricular systolic strain and systolic strain rate, and tricuspid annular plane systolic excursion were reported as risk stratification indicators for the patients with AL amyloidosis, with the two-fold purpose of risk stratification and early detection of cardiac dysfunction [105]. However, morphological (left ventricular hypertrophy, index interventricular septum thickness) as well as functional (mitral annular systolic velocity, mitral/tricuspid annular plane systolic excursion) findings by echocardiography, and LGE by CMR failed to stratify the risk of patients with ATTR in another study [106]. And ECV showed that a higher risk for death existed with ECV $>$ 0.45 compared with patients with ECV $<$ 0.45 in a 23-month follow-up study [107]. It seems doubtful that LGE was not a risk factor as visualization of cardiac amyloid infiltration with LGE imaging and measurements of cardiac amyloid burden with ECV were all previously proven, yet these were not investigated systematically in risk stratification of CA and it remains a relatively unexplored research area.

In view of the clinical and prognostic significance of CA, several noninvasive diagnostic tools have been reported for predicting AL amyloidosis mortality, including ECG and echocardiography [108–110], cardiac biomarkers such as cTnT and NT-proBNP provide potent prognostic value in patients with AL amyloidosis [111]. In recent years, with the development of LGE and T1 mapping, CMR imaging has increasingly been used not just for early and accurate diagnosis but also prognosis evaluation, and positive and diffuse LGE provides incremental prognostic value over clinical, laboratory and echocardiographic variables for mortality prediction in

AL amyloidosis patients with endomyocardial biopsy as the gold standard [61,12].

LGE is a predictor of outcome in almost all cardiac conditions except amyloidosis where studies have shown paradoxical results. This may be partially explained by the use of non-standardized LGE approaches [29,112] as well as difficult identification of diffuse LGE and error-prone choice of inversion time. Transmural LGE with PSIR sequence represents advanced CA and is relevant with high ECV and poor prognosis while associating the observed LGE pattern (normal, sub-endocardial, transmural) with ECV and clinical outcomes [63]. Additionally, a modified LGE protocol of increasing inversion times identified patients with histologically-proven CA accurately and was a robust predictor of death with presence of diffuse hyper-enhancement [112]. Notably, ECV $>$ 0.58 was independently correlated with mortality in all patients with cardiac ATTR, as well as those with mTTR and wtTTR [84].

Patients with AL amyloidosis had a significantly worse prognosis compared with ATTR amyloidosis (median overall survival: 15.7–18 months vs. $\geq$38.9–45 months) [32,113]. Since there is more extensive LGE with right ventricular involvement in individuals with ATTR than in those with AL according to Dungu et al's study [31], increased LGE and increased interstitial expansion may not be prognostic factors of amyloidosis because ATTR is associated with a better prognosis than AL [114].

Besides the prognostic value of LGE and T1 mapping on CA, some relevant research on cardiac function with CMR also showed promising potential. Early, left atrial emptying fraction was found to be inversely associated with highly sensitive cTnT, an established risk marker for mortality [115]. Then, increased left atrial volume and reduced left atrial emptying fraction were associated with well-established risk factors for mortality in a large cohort study of 1802 participants [115] and 44 consecutive patients with confirmed AL amyloidosis [116]. Those at moderate and high risk had significantly larger indexed maximum left atrial volume and indexed minimal left atrial volume, lower left atrial emptying fraction compared with patients with no or minimal cardiac involvement [116]. There is no published data on evaluation of right ventricular function with CMR to risk stratify CA patients, but right ventricular dilation measured by echocardiography was studied and correlated with more severe cardiac involvement and shorter survival [110].

Disease tracking

Disease tracking is important after therapy. Cardiac morphology and function have limited value in evaluating therapy response in AL amyloidosis [117], in contrast to ATTR amyloidosis [118]. LGE imaging demonstrated marked regression of the subendocardial hyperenhancement after stem cell transplantation after 2.5 years in a case report [117]. These all need to be further studied with larger samples.

T1 mapping, including native T1 mapping and ECV, has high potential to follow disease changes in patients with CA over time at three different levels: amyloid infiltration (ECV), edema (native T1), and myocyte response (intracellular volume), offering a broader understanding of the pathophysiology of the treatment response [29]. A few studies evaluated T1 mapping in clinical follow-up as a marker of response to treatment. A reduction in native T1 values after treatment in both AL and ATTR amyloidosis, in conjunction with overall reduction in systemic and cardiac biomarkers in the setting of clinical improvement with treatment, may represent regression of amyloid deposition in the myocardium [118,119].

CMR functional parameters, including myocardial strain and myocardial perfusion, are also used to track cardiovascular responses in patients with dialysis related amyloidosis [120]. Buchanan et al. [120] used a crossover study with CMR between patients on standard hemodialysis and hemodiafiltration, also called intradialytic CMR, to examine the comparative acute cardiovascular effects of standard hemodialysis versus hemofiltration in 12 stable patients with dialysis-related amyloidosis. There was no significant difference in the cardiovascular response between these two treatment modalities except decreased systolic contractile function calculated by cardiac deformation imaging and significantly decreased myocardial perfusion during standard hemodialysis and hemodiafiltration. Besides, global longitudinal systolic strain with echocardiography identified short-term improvement after chemotherapy for AL amyloidosis, which can better predict survival than cardiac biomarkers [72].

ECV measurement has already been considered sufficiently potent in some AL amyloidosis diagnostic and prognostic assessment studies, however, no concerning studies were reported on disease change after treatment over time so far, which may need further exploration. A prospective study tracked cardiac response with serum levels of NT-proBNP after monoclonal antibody targeting treatment in patients with AL amyloidosis and persistent organ dysfunction [121], but by far no prospective clinical outcome studies demonstrated the value of CMR in evaluating cardiac response to treatment, or in directing appropriate treatment of cardiac amyloidosis.

The future of CMR for amyloidosis

Over many decades, advances in echocardiography, nuclear imaging, and CMR have been coupled with research in CA. In part, because of the diffuse nature of the cardiac involvement and the fact that there is a combination of clinical and imaging features that have been accepted as being diagnostic short of myocardial biopsy, multimodality imaging in amyloidosis will continue to have an impact on clinical care.

Apart from the emerging of new CMR techniques, Xu et al. [122] proposed an end-to-end deep-learning algorithm framework to accurately detect the myocardial infarction area at the pixel level in 114 clinical patients using CMR images, yielding an overall classification accuracy of 94.35% at the pixel level. It opens a new chapter of radiomics in CMR and may improve diagnosis of CA in the big data era.

Rather than being mostly an imaging diagnosis, the imaging advances will be more closely aligned with therapies as molecular imaging (including PET/MR), serum and imaging biomarkers, quantification of myocardial involvement, functional, hemodynamic, and clinical status are linked to innovative and transformative therapies. Some tissue characterization like ECV and new CMR techniques such as myocardial strain might also play a future role in tracking treatment, as proposed in recent work in patients with severe aortic stenosis [123].

In recent years, the field of CMR diffusion tensor imaging (DTI) has gained significant momentum. The integrity, mobility and arrangement of the myocytes contribute significantly to efficient ventricular function [124], and cardiac DTI has shown potential to gain novel insights into various cardiac conditions including myocardial infarction and cardiomyopathy [125,126]. Though the application of DTI in CA has not been reported, it turns to be a promising prospective to study since DTI is now widely applied for assessment of amyloid in the brain [127–129]. Some limitations of cardiac DTI-tractography include its spatial resolution and inability to resolve molecular signatures in the tissue imaged [130], but constant efforts in the technology have been made to overcome the shortcomings of the diffusion tensor to reduced repetition time, increased signal-to-noise ratio and free-breathing imaging [131,132].

Lastly, animal models to study CA are limited by the type of model [133–135]. Only one study on therapy effect [136] and no report about CMR in animal models of CA has been published until now.

Cardiac involvement in systemic amyloidosis has both therapeutic and prognostic significance, it is crucial to make a diagnosis quantitatively and qualitatively, or provide prognostic value objectively. In summary, amyloid cardiomyopathy has to be investigated before heart failure and cardiac MRI is recommended routinely in patients for comprehensively assessment in cardiac morphology, function, risk stratification, prognosis, and guidance of therapy. The single modality-based diagnosis has been replaced by an integrated multimodality approach, and there is ample evidence that CMR holds value in CA. However, as the field of medicine continues to improve quality and value, the field of CMR must necessarily evolve as well.

References

[1] Czeyda-Pommersheim F, Hwang M, Chen SS, Strollo D, Fuhrman C, Bhalla S. Amyloidosis: modern cross-sectional imaging. Radiographics 2015;35:1381–92.

[2] D'Souza A, Dispenzieri A, Wirk B, Zhang MJ, Huang J, Gertz MA, et al. Improved outcomes after autologous hematopoietic cell transplantation for light chain amyloidosis: a center for international blood and marrow transplant research study. J Clin Oncol 2015;33:3741–9.

[3] Castaño A, Drachman BM, Judge D, Maurer MS. Natural history and therapy of TTR-CA: emerging disease-modifying therapies from organ transplantation to stabilizer and silencer drugs. Heart Fail Rev 2015;20:163–78.

[4] Muchtar E, Gertz MA, Kumar SK, Lacy MQ, Dingli D, Buadi FK, et al. Improved outcomes for newly diagnosed AL amyloidosis over the years 2000 and 2014: cracking the glass ceiling of early death. Blood 2017;129:2111–19.

[5] Fontana M, Banypersad SM, Treibel TA, Maestrini V, Sado DM, White SK, et al. Native T1 mapping in transthyretin amyloidosis. JACC Cardiovasc Imaging 2014;7:157–65.

[6] Gertz MA, Benson MD, Dyck PJ, Grogan M, Coelho T, Cruz M, et al. Diagnosis, prognosis, and therapy of transthyretin amyloidosis. J Am Coll Cardiol 2015;66:2451–66.

[7] Ruberg FL, Berk JL. Transthyretin (TTR) cardiac amyloidosis. Circulatio 2012;126:1286–300.

[8] Siddiqi OK, Ruberg FL. Challenging the myths of cardiac amyloidosis. Eur Heart J 2017;38:1909–12.

[9] Wechalekar AD, Gillmore JD, Hawkins PN. Systemic amyloidosis. Lancet 2016;387:2641–54.

[10] Palladini G, Merlini G. What is new in diagnosis and management of light chain amyloidosis? Blood 2016;128:159–68.

[11] Mohty D, Damy T, Cosnay P, Echahidi N, Casset-Senon D, Virot P, et al. Cardiac amyloidosis: updates in diagnosis and management. Arch Cardiovasc Dis 2013;106:528–40.

[12] Alkhawam H, Patel D, Nguyen J, Easaw SM, Al-Sadawi M, Syed U, et al. Cardiac amyloidosis: pathogenesis, clinical context, diagnosis and management options. Acta Cardiol 2017;72:380–9.

[13] Longhi S, Guidalotti PL, Quarta CC, Gagliardi C, Milandri A, Lorenzini M, et al. Identification of TTR-related subclinical amyloidosis with 99mTc-DPD scintigraphy. JACC Cardiovasc Imaging 2014;7:531–2.

[14] Bhatti S, Watts E, Syed F, Vallurupalli S, Pandey T, Jambekar K, et al. Clinical and prognostic utility of cardiovascular magnetic resonance imaging in myeloma patients with suspected cardiac amyloidosis. Eur Heart J Cardiovasc Imaging 2016;17:970–7.

[15] Falk RH, Quarta CC, Dorbala S. How to image cardiac amyloidosis. Circ Cardiovasc Imaging 2014;7:552–62.

[16] Grogan M, Dispenzieri A, Gertz MA. Light-chain cardiac amyloidosis: strategies to promote early diagnosis and cardiac response. Heart 2017;103:1065–72.

[17] Gertz MA, Dispenzieri A, Sher T. Pathophysiology and treatment of cardiac amyloidosis. Nat Rev Cardiol 2015;12:91–102.

[18] Knight DS, Zumbo G, Barcella W, Steeden JA, Muthurangu V, Martinez-Naharro A, et al. Cardiac structural and functional consequences of amyloid deposition by cardiac magnetic resonance and echocardiography and their prognostic roles. JACC Cardiovasc Imaging 2018 [Epub ahead of print]). doi:10.1016/j.jcmg.2018.02.016.

[19] Fontana M, Chung R, Hawkins PN, Moon JC. Cardiovascular magnetic resonance for amyloidosis. Heart Fail Rev 2015;20:133–44.

[20] Flachskampf FA, Biering-Sørensen T, Solomon SD, Duvernoy O, Bjerner T, Smiseth OA. Cardiac imaging to evaluate left ventricular diastolic function. JACC Cardiovasc Imaging 2015;8:1071–93.

[21] Wollmann CG, Thudt K, Kaiser B, Salomonowitz E, Mayr H, Globits S. Safe performance of magnetic resonance of the heart in patients with magnetic resonance conditional pacemaker systems: the safety issue of the ESTIMATE study. J Cardiovasc Magn Reson 2014;16:30.

[22] Bailey WM, Rosenthal L, Fananapazir L, Gleva M, Mazur A, Rinaldi CA, et al. Clinical safety of the ProMRI pacemaker system in patients subjected to head and lower lumbar 1.5-T magnetic resonance imaging scanning conditions. Heart Rhythm 2015;12:1183–91.

[23] Gold MR, Sommer T, Schwitter J, Al Fagih A, Albert T, Merkely B, et al. Full–body MRI in patients with an implantable cardioverter-defibrillator: primary results of a randomized study. J Am Coll Cardiol 2015;65(24):2581–8.

[24] Wilkoff BL, Bello D, Taborsky M, Vymazal J, Kanal E, Heuer H, et al. Magnetic resonance imaging in patients with a pacemaker system designed for the magnetic resonance environment. Heart Rhythm 2011;8:65–73.

[25] Do DH, Eyvazian V, Bayoneta AJ, Hu P, Finn JP, Bradfield JS, et al. Cardiac magnetic resonance imaging using wideband sequences in patients with nonconditional cardiac implanted electronic devices. Heart Rhythm 2018;15:218–225.

[26] Levine GN, Gomes AS, Arai AE, Bluemke DA, Flamm SD, Kanal E, et al. Safety of magnetic resonance imaging in patients with cardiovascular devices an American Heart Association scientific statement from the Committee on Diagnostic and Interventional Cardiac Catheterization, Council on Clinical Cardiology, and the Council on Cardiovascular Radiology and Intervention: endorsed by the American College of Cardiology Foundation, the North American Society for Cardiac Imaging, and the Society for Cardiovascular Magnetic Resonance. Circulation 2007;116:2878–91.

[27] Russo RJ, Costa HS, Silva PD, Anderson JL, Arshad A, Biederman RW, et al. Assessing the risks associated with MRI in patients with a pacemaker or defibrillator. N Engl J Med 2017;376:755–64.

[28] Strom JB, Whelan JB, Shen C, Zheng SQ, Mortele KJ, Kramer DB. Safety and utility of magnetic resonance imaging in patients with cardiac implantable electronic devices. Heart Rhythm 2017;14:1138–44.

[29] Palladini G, Milani P, Merlini G. Novel strategies for the diagnosis and treatment of cardiac amyloidosis. Expert Rev Cardiovasc Ther 2015;13:1195–211.

[30] Roller FC, Harth S, Schneider C, Krombach GA. T1, T2 mapping and extracellular volume fraction (ECV): application, value and further perspectives in myocardial inflammation and cardiomyopathies. Rofo 2015;187:760–70.

[31] Fontana M, Banypersad SM, Treibel TA, Abdel-Gadir A, Maestrini V, Lane T, et al. Differential myocyte responses in patients with cardiac transthyretin amyloidosis and light-chain amyloidosis: a cardiac MR imaging study. Radiology 2015;277:388–97.

[32] Dungu JN, Valencia O, Pinney JH, Gibbs SD, Rowczenio D, Gilbertson JA, et al. CMR-based differentiation of AL and ATTR cardiac amyloidosis. JACC Cardiovasc Imaging 2014;7:133–42.

[33] Ruberg FL, Nezafat R. Cardiovascular magnetic resonance visualization of cardiac amyloid infiltration: challenges and opportunities. Circulation 2015;132:1525–7.

[34] Ordovas KG, Higgins CB. Delayed contrast enhancement on MR images of myocardium: past, present, future. Radiology 2011;261:358–74.

[35] Syed IS, Glockner JF, Feng D, Araoz PA, Martinez MW, Edwards WD, et al. Role of cardiac magnetic resonance imaging in the detection of cardiac amyloidosis. JACC Cardiovasc Imaging 2010;3:155–64.

[36] van Oorschot JW, Gho JM, van Hout GP, Froeling M, Jansen Of Lorkeers SJ, Hoefer IE, Doevendans PA, et al. Endogenous contrast MRI of cardiac fibrosis: beyond late gadolinium enhancement. J Magn Reson Imaging 2014;41:1181–1189.

[37] Banypersad SM, Fontana M, Maestrini V, Sado DM, Captur G, Petrie A, et al. T1 mapping and survival in systemic light-chain amyloidosis. Eur Heart J 2015;36:244–51.

[38] Tuzovic M, Yang EH, Baas AS, Depasquale EC, Deng MC, Cruz D, et al. Cardiac amyloidosis: diagnosis and treatment strategie. Curr Oncol Rep 2017;19:46.

[39] Muscogiuri G, Suranyi P, Schoepf UJ, De Cecco CN, Secinaro A, Wichmann JL, et al. Cardiac magnetic resonance T1-mapping of the myocardium technical background and clinical relevance. J Thorac Imaging 2018;33:71–80.

[40] Qian J, Huo J, Qian J, Gao T, Gou Y. Novel potential therapeutic strategies of senile cardiac amyloidosis: heat shock factor 1 blocks senile cardiac amyloidosis via HSPA1A in mouse model. Int J Cardiol 2015;195:285–7.

[41] Fikrle M, Palecek T, Masek M, Kuchynka P, Straub J, Spicka I, et al. The diagnostic performance of cardiac magnetic resonance in detection of myocardial involvement in AL amyloidosis. Clin Physiol Funct Imaging 2016;36:218–24.

[42] Kellman P, Xue H, Olivieri LJ, Cross RR, Grant EK, Fontana M, et al. Dark blood late enhancement imaging. J Cardiovasc Magn Reson 2016;18:77.

[43] Basha TA, Tang MC, Tsao C, Tschabrunn CM, Anter E, Manning WJ, et al. Improved dark blood late gadolinium enhancement (DB-LGE) imaging using an optimized jointinversion preparation and T2 magnetization preparation. Magn Reson Med 2018;79:351–60.

[44] Kido T, Kido T, Nakamura M, Kawaguchi N, Nishiyama Y, Ogimoto A, et al. Three-dimensional phase-sensitive inversion recovery sequencing in the evaluation of left ventricular myocardial scars in ischemic and non-ischemic cardiomyopathy: comparison to threedimensional inversion recovery sequencing. Eur J Radiol 2014;83:2159–66.

[45] Ginami G, Neji R, Rashid I, Chiribiri A, Ismail TF, Botnar RM, et al. 3D whole–heart phase sensitive inversion recovery CMR for simultaneous black-blood late gadolinium enhancement and bright-blood coronary CMR angiography. J Cardiovasc Magn Reson 2017;19:94.

[46] Maurer MS, Elliott P, Comenzo R, Semigran M, Rapezzi C. Addressing common questions encountered in the diagnosis and management of cardiac amyloidosis. Circulation 2017;135:1357–77.

[47] Messroghli DR, Radjenovic A, Kozerke S, Higgins DM, Sivananthan MU, Ridgway JP. Modified Look-Locker inversion recovery (MOLLI) for high-resolution T1 mapping of the heart. Magn Reson Med 2004;52:141–6.

[48] Piechnik SK, Ferreira VM, Dall'Armellina E, Cochlin LE, Greiser A, Neubauer S, et al. Shortened Modified Look-Locker Inversion recovery (ShMOLLI) for clin-

ical myocardial T1-mapping at 1.5 and 3 T within a 9 heartbeat breathhold. J Cardiovasc Magn Reson 2010;12:69.
[49] Chow K, Flewitt JA, Green JD, Pagano JJ, Friedrich MG, Thompson RB. Saturation recovery single-shot acquisition (SASHA) for myocardial T(1) mapping. Magn Reson Med 2014;71:2082–95.
[50] Weingärtner S, Akçakaya M, Basha T, Kissinger KV, Goddu B, Berg S, et al. Combined saturation/inversion recovery sequences for improved evaluation of scar and diffuse fibrosis in patients with arrhythmia or heart rate variability. Magn Reson Med 2014;71:1024–34.
[51] Liu CY, Liu YC, Wu C, Armstrong A, Volpe GJ, van der Geest RJ, et al. Evaluation of age-related interstitial myocardial fibrosis with cardiac magnetic resonance contrast-enhanced T1 mapping: MESA (Multi-Ethnic Study of Atherosclerosis). J Am Coll Cardiol 2013;62:1280–7.
[52] Karamitsos TD, Piechnik SK, Banypersad SM, Fontana M, Ntusi NB, Ferreira VM, et al. Noncontrast T1 mapping for the diagnosis of cardiac amyloidosis. JACC Cardiovasc Imaging 2013;6:488–97.
[53] Ntusi NA, Piechnik SK, Francis JM, Ferreira VM, Rai AB, Matthews PM, et al. Subclinical myocardial inflammation and diffuse fibrosis are common in systemic sclerosis–a clinical study using myocardial T1-mapping and extracellular volume quantification. J Cardiovasc Magn Reson 2014;16:21.
[54] Thompson RB, Chow K, Khan A, Chan A, Shanks M, Paterson I, et al. T1 mapping with cardiovascular MRI is highly sensitive for Fabry disease independent of hypertrophy and sex. Circ Cardiovasc Imaging 2013;6:637–45.
[55] Roujol S, Weingartner S, Foppa M, Chow K, Kawaji K, Ngo LH, et al. Accuracy, precision, and reproducibility of four T1 mapping sequences: a head--tohead comparison of MOLLI, ShMOLLI, SASHA, and SAPPHIRE. Radiology 2014;272:683–9.
[56] Puntmann VO, Voigt T, Chen Z, Mayr M, Karim R, Rhode K, et al. Native T1 mapping in differentiation of normal myocardium from diffuse disease in hypertrophic and dilated cardiomyopathy. JACC Cardiovasc Imaging 2013;6:475–84.
[57] Dass S, Suttie JJ, Piechnik SK, Ferreira VM, Holloway CJ, Banerjee R, et al. Myocardial tissue characterization using magnetic resonance noncontrast t1 mapping in hypertrophic and dilated cardiomyopathy. Circ Cardiovasc Imaging 2012;5:726–33.
[58] Rao AK, Greve AM, Nielles-Vallespin S. Variability of T1 in purpose recruited normal volunteers and patients as a function of shim (B0), flip angle (B1) and myocardial sector at 3T. J Cardiovasc Magn Reson 2015;17:P5.
[59] Weingärtner S, Meßner NM, Budjan J, Loßnitzer D, Mattler U, Papavassiliu T, et al. Myocardial T1-mapping at 3T using saturation-recovery: reference values, precision and comparison with MOLLI. J Cardiovasc Magn Reson 2016;18:84.
[60] aus dem Siepen F, Buss SJ, Messroghli D, Andre F, Lossnitzer D, Seitz S, et al. T1 mapping in dilated cardiomyopathy with cardiac magnetic resonance: quantification of diffuse myocardial fibrosis and comparison with endomyocardial biopsy. Eur Heart J Cardiovasc Imaging 2015;16:210–16.
[61] Sado DM, White SK, Piechnik SK, Banypersad SM, Treibel TA, Captur G, et al. Identification and assessment of Anderson-Fabry disease by cardiovascular magnetic resonance noncontrast myocardial T1 mapping. Circ Cardiovasc Imaging 2013;6:392–8.
[62] Boynton SJ, Geske JB, Dispenzieri A, Syed IS, Hanson TJ, Grogan M, et al. LGE provides incremental prognostic information over serum biomarkers in AL cardiac amyloidosis. JACC Cardiovasc Imaging 2016;9:680–6.
[63] Fontana M, Pica S, Reant P, Abdel-Gadir A, Treibel TA, Banypersad SM, et al. Prognostic value of late gadolinium enhancement cardiovascular magnetic resonance in cardiac amyloidosis. Circulation 2015;132:1570–9.
[64] Lee JJ, Liu S, Nacif MS, Ugander M, Han J, Kawel N, et al. Myocardial T1 and extracellular volume fraction mapping at 3 tesla. J Cardiovasc Magn Reson 2011;13:75–85.
[65] Kellman P, Arai AE, Xue H. T1 and extracellular volume mapping in the heart: estimation of error maps and the influence of noise on precision. J Cardiovasc Magn Reson 2013;15:56.
[66] Gillmore JD, Maurer MS, Falk RH, Merlini G, Damy T, Dispenzieri A, et al. Nonbiopsy diagnosis of cardiac transthyretin amyloidosis. Circulation 2016;133:2404–12.
[67] Trivieri MG, Dweck MR, Abgral R, Robson PM, Karakatsanis NA, Lala A, et al. 18F-sodium fluoride PET/MR for the assessment of cardiac amyloidosis. J Am Coll Cardiol 2016;68:2712–14.
[68] Piper C, Butz T, Farr M, Faber L, Oldenburg O, Horstkotte D. How to diagnose cardiac amyloidosis early: impact of ECG, tissue Doppler echocardiography, and myocardial biopsy. Amyloid 2010;17:1–9.
[69] Liu D, Hu K, Niemann M, Herrmann S, Cikes M, Stork S, et al. Effect of combined systolic and diastolic functional param- eter assessment for differentiation of cardiac amyloidosis from other causes of concentric left ventricular hypertrophy. Circ Cardiovasc Imaging 2013;6:1066–72.
[70] Senapati A, Sperry BW, Grodin JL, Kusunose K, Thavendiranathan P, Jaber W, et al. Prognostic implication of relative regional strain ratio in cardiac amyloidosis. Heart 2016;102:748–54.
[71] Barros-Gomes S, Williams B, Nhola LF, Grogan M, Maalouf JF, Dispenzieri A, et al. Prognosis of light chain amyloidosis with preserved LVEF: added value of 2D speckle-tracking echocardiography to the current prognostic staging system. JACC Cardiovasc Imaging 2017;10:398–407.
[72] Salinaro F, Meier-Ewert HK, Miller EJ, Pandey S, Sanchorawala V, Berk JL, et al. Longitudinal systolic strain, cardiac function improvement, and survival following treatment of light-chain (AL) cardiac amyloidosis. Eur Heart J Cardiovasc Imaging 2017;18:1057–64.
[73] Meng L, Lin K, Collins J, Markl M, Carr JC. Automated description of regional left ventricular motion in patients with cardiac amyloidosis: a quantitative study using heart deformation analysis. AJR Am J Roentgenol 2017;209:W57–63.
[74] Quarta CC, Solomon SD, Uraizee I, Kruger J, Longhi S, Ferlito M, et al. Left ventricular structure and function in transthyretinrelated versus light-chain cardiac amyloidosis. Circulation 2014;129:1840–9.
[75] Cappelli F, Porciani MC, Bergesio F, Perfetto F, De Antoniis F CaniaA, et al. Characteristics of left ventricular rotational mechanics in patients with systemic amyloidosis systemic hypertension and normal left ventricular mass. Clin Physiol Funct Imaging 2011;31:159–65.
[76] Oda S, Utsunomiya D, Nakaura T, Yuki H, Kidoh M, Morita K, et al. Identification and assessment of cardiac amyloidosis by myocardial strain analysis of cardiac magnetic resonance imaging. Circ J 2017;81:1014–21.
[77] Arani A, Arunachalam SP, Chang IC, Baffour F, Rossman PJ, Glaser KJ, et al. Cardiac MR elastography for quantitative assessment of elevated myocardial stiffness in cardiac amyloidosis. J Magn Reson Imaging 2017;46:1361–7.
[78] Chang ICY, Arani A, Poigai Arunachalam S, Grogan M, Dispenzieri A, Araoz PA. Feasibility study of cardiac magnetic resonance elastography in cardiac amyloidosis. Amyloid 2017;24(sup1):161.
[79] Rapezzi C, Merlini G, Quarta CC, Riva L, Longhi S, Leone O, et al. Systemic cardiac amyloidoses: disease profiles and clinical courses of the 3 main types. Circulation 2009;120:1203–12.
[80] Damy T, Costes B, Hagège AA, Donal E, Eicher JC, Slama M, et al. Prevalence and clinical phenotype of hereditary transthyretin amyloid cardiomyopathy in patients with increased left ventricular wall thickness. Eur Heart J 2016;37:1826–34.
[81] Li R, Yang ZG, Wen LY, Liu X, Xu HY, Zhang Q, et al. Regional myocardial microvascular dysfunction in cardiac amyloid light-chain amyloidosis: assessment with 3T cardiovascular magnetic resonance. J Cardiovasc Magn Reson 2016;18:16.
[82] Li R, Yang ZG, Xu HY, Shi K, Liu X, Diao KY, et al. Myocardial deformation in cardiac amyloid light-chain amyloidosis: assessed with 3T cardiovascular magnetic resonance feature tracking. Sci Rep 2017;7:3794.
[83] Siddiqi OK, Ruberg FL. Cardiac amyloidosis: an update on pathophysiology, diagnosis, and treatment. Trends Cardiovasc Med 2018;28:10–21.
[84] Martinez-Naharro A, Treibel TA, Abdel-Gadir A, Bulluck H, Zumbo G, Knight DS, et al. Magnetic resonance in transthyretin cardiac amyloidosis. J Am Coll Cardiol 2017;70:466–77.
[85] Pozo E, Kanwar A, Deochand R, Castellano JM, Naib T, Pazos-López P, et al. Cardiac magnetic resonance evaluation of left ventricular remodelling distribution in cardiac amyloidosis. Heart 2014;100:1688–95.
[86] Fine NM, Arruda-Olson AM, Dispenzieri A, Zeldenrust SR, Gertz MA, Kyle RA, et al. Yield of noncardiac biopsy for the diagnosis of transthyretin cardiac amyloidosis. Am J Cardiol 2014;113:1723–7.
[87] Cariou E, Bennani Smires Y, Victor G, Robin G, Ribes D, Pascal P, et al. Diagnostic score for the detection of cardiac amyloidosis in patients with left ventricular hypertrophy and impact on prognosis. Amyloid 2017;24:101–9.
[88] Kwong RY, Heydari B, Abbasi S, Steel K, Al-Mallah M, Wu H, et al. Characterization of cardiac amyloidosis by atrial late gadolinium enhancement using contrast-enhanced cardiac magnetic resonance imaging and correlation with left atrial conduit and contractile function. Am J Cardiol 2015;116:622–9.
[89] Deux JF, Damy T, Rahmouni A, Mayer J, Planté-Bordeneuve V. Noninvasive detection of cardiac involvement in patients with hereditary transthyretin associated amyloidosis using cardiac magnetic resonance imaging: a prospective study. Amyloid 2014;21:246–55.
[90] Ferreira VM, Piechnik SK, Dall'Armellina E, Karamitsos TD, Francis JM, Choudhury RP, et al. Non contrast T1 mapping detects acute myocardial edema with high diagnostic accuracy: a comparison to T2-weighted cardiovascular magnetic resonance. J Cardiovasc Magn Reson 2012;14:42.
[91] Ruberg FL. T1 mapping in cardiac amyloidosis: can we get there from here? J Am Coll Cardiol Img 2013;6:498–500.
[92] Oda S, Utsunomiya D, Morita K, Nakaura T, Yuki H, Kidoh M, et al. Cardiovascular magnetic resonance myocardial T1 mapping to detect and quantify cardiac involvement in familial amyloid polyneuropathy. Eur Radiol 2017;27:4631–8.
[93] Tuzovic M, Yang EH, Baas AS, Depasquale EC, Deng MC, Cruz D, et al. Cardiac amyloidosis: diagnosis and treatment strategie. Curr Oncol Rep 2017;19:46.
[94] Sado DM, Flett AS, Banypersad SM, White SK, Maestrini V, Quarta G, et al. Cardiovascular magnetic resonance measurement of myocardial extracellular volume in health and disease. Heart 2012;98:1436–41.
[95] Barison A, Aquaro GD, Pugliese NR, Cappelli F, Chiappino S, Vergaro G, et al. Measurement of myocardial amyloid deposition in systemic amyloidosis: insights from cardiovascular magnetic resonance imaging. J Intern Med 2015;277:605–14.
[96] Banypersad SM, Sado DN, Flett AS, Gibbs SD, Pinney JH, Maestrini V, et al. Quantification of myocardial extracellular volume fraction in systemic AL amyloidosis: an equilibrium contrast cardiovascular magnetic resonance study. Circ Cardiovasc Imaging 2013;6:34–9.

[97] Fontana M, Banypersad S, Treibel TA, Maestrini V, Sado DN, White SK, et al. AL and ATTR cardiac amyloid are different: native T1 mapping and ECV detect different biology. J Cardiovasc Magn Reson 2014;16(Suppl 1):P341.
[98] Merlini G, Lousada I, Ando Y, Dispenzieri A, Gertz MA, Grogan M, et al. Rationale, application and clinical qualification for NT-proBNP as a surrogate end point in pivotal clinical trials in patients with AL amyloidosis. Leukemia 2016;30:1979–86.
[99] Dispenzieri A, Gertz MA, Kyle RA, Lacy MQ, Burritt MF, Therneau TM, et al. Serum cardiac troponins and N-terminal probrain natriuretic peptide: a staging system for primary systemic amyloidosis. J Clin Oncol 2004;22:3751–7.
[100] Kumar S, Dispenzieri A, Lacy MQ, Hayman SR, Buadi FK, Colby C, et al. Revised prognostic staging system for light chain amyloidosis incorporating cardiac biomarkers and serum free light chain measurements. J Clin Oncol 2012;30:989–95.
[101] Grogan M, Scott CG, Kyle RA, Zeldenrust SR, Gertz MA, Lin G, et al. Natural history of wild-type transthyretin cardiac amyloidosis and risk stratification using a novel staging system. J Am Coll Cardiol 2016;68:1014–20.
[102] Dispenzieri A, Gertz MA, Kumar SK, Lacy MQ, Kyle RA, Saenger AK, et al. High sensitivity cardiac troponin T in patients with immunoglobulin light chain amyloidosis. Heart 2014;100:383–8.
[103] Kumar SK, Gertz MA, Lacy MQ, Dingli D, Hayman SR, Buadi FK, et al. Recent improvements in survival in primary systemic amyloidosis and the importance of an early mortality risk score. Mayo Clin Proc 2011;86:12–18.
[104] Grogan M, Scott CG, Kyle RA, Zeldenrust SR, Gertz MA, Lin G, et al. Natural history of wild-type transthyretin cardiac amyloidosis and risk stratification using a novel staging system. J Am Coll Cardiol 2016;68:1014–20.
[105] Bellavia D, Pellikka PA, Dispenzieri A, Scott CG, Al-Zahrani GB, Grogan M, et al. Comparison of right ventricular longitudinal strain imaging, tricuspid annular plane systolic excursion, and cardiac biomarkers for early diagnosis of cardiac involvement and risk stratification in primary systematic (AL) amyloidosis: a 5-year cohort study. Eur Heart J Cardiovasc Imaging 2012;13:680–689.
[106] Kristen AV, Scherer K, Buss S, aus dem Siepen F, Haufe S, Bauer R, et al. Noninvasive risk stratification of patients with transthyretin amyloidosis. JACC Cardiovasc Imaging 2014;7:502–10.
[107] Banypersad SM, Fontana M, Maestrini V, Sado DM, Captur G, Petrie A, et al. T1 mapping and survival in systemic light-chain amyloidosis. Eur Heart J 2015;36:244–51.
[108] Mussinelli R, Salinaro F, Alogna A, Boldrini M, Raimondi A, Musca F, et al. Diagnostic and prognostic value of low QRS voltages in cardiac AL amyloidosis. Ann Noninvasive Electrocardiol 2013;18:271–80.
[109] Buss SJ, Emami M, Mereles D, Korosoglou G, Kristen AV, Voss A, et al. Longitudinal left ventricular function for prediction of survival in systemic light-chain amyloidosis: incremental value compared with clinical and biochemical markers. J Am Coll Cardiol 2012;60:1067–76.
[110] Ghio S, Perlini S, Palladini G, Marsan NA, Faggiano G, Vezzoli M, et al. Importance of the echocardiographic evaluation of right ventricular function in patients with AL amyloidosis. Eur J Heart Fail 2007;9:808–13.
[111] Kristen AV, Giannitsis E, Lehrke S, Hegenbart U, Konstandin M, Lindenmaier D, et al. Assessment of disease severity and outcome in patients with systemic light-chain amyloidosis by the high-sensitivity troponin T assay. Blood 2010;116:2455–61.
[112] White JA, Kim HW, Shah D, Fine N, Kim KY, Wendell DC, et al. CMR imaging with rapid visual T1 assessment predicts mortality in patients suspected of cardiac amyloidosis. JACC Cardiovasc Imaging 2014;7:143–56.
[113] Rapezzi C, Quarta CC, Obici L, Perfetto F, Longhi S, Salvi F, et al. Disease profile and differential diagnosis of hereditary transthyretin-related amyloidosis with exclusively cardiac phenotype: an Italian perspective. Eur Heart J 2013;34:520–8.
[114] Hashimura H, Kimura F, Ishibashi-Ueda H, Morita Y, Higashi M, Nakano S, et al. Radiologic-pathologic correlation of primary and secondary cardiomyopathies: MR imaging and histopathologic findings in hearts from autopsy and transplantation. Radiographics 2017;37:719–36.
[115] Gupta S, Matulevicius SA, Ayers CR, Berry JD, Patel PC, Markham DW, et al. Left atrial structure and function and clinical outcomes in the general population. Eur Heart J 2013;34:278–85.
[116] Mohty D, Boulogne C, Magne J, Varroud-Vial N, Martin S, Ettaif H, et al. Prognostic value of left atrial function in systemic light-chain amyloidosis: a cardiac magnetic resonance study. Eur Heart J Cardiovasc Imaging 2016;17:961–9.
[117] Brahmanandam V, McGraw S, Mirza O, Desai AA, Farzaneh-Far A. Regression of cardiac amyloidosis after stem cell transplantation assessed by cardiovascular magnetic resonance imaging. Circulation 2014;129:2326–8.
[118] aus dem Siepen F, Buss SJ, Andre F, Seitz S, Giannitsis E, Steen H, et al. Extracellular remodeling in patients with wild-type amyloidosis consuming epigallocatechin-3-gallate: preliminary results of T1 mapping by cardiac magnetic resonance imaging in a small single center study. Clin Res Cardiol 2015;104:640–7.
[119] Hur DJ, Dicks DL, Huber S, Mojibian HR, Meadows JL, Seropian SE, et al. Serial native T1 mapping to monitor cardiac response to treatment in light-chain amyloidosis. Circ Cardiovasc Imaging 2016;9 pii: e004770.
[120] Buchanan C, Mohammed A, Cox E, Köhler K, Canaud B, Taal MW, et al. Intradialytic cardiac magnetic resonance imaging to assess cardiovascular responses in a short-term trial of hemodiafiltration and hemodialysis. J Am Soc Nephrol 2017;28:1269–77.
[121] Gertz MA, Landau H, Comenzo RL, Seldin D, Weiss B, Zonder J, et al. First-in-human phase I/II study of NEOD001 in patients with light chain amyloidosis and persistent organ dysfunction. J Clin Oncol 2016;34:1097–103.
[122] Chenchu Xu, Lei Xu, Zhifan Gao, Shen zhao, Heye Zhang, et al. Direct detection of pixel-level myocardial infarction areas via a deep-learning algorithm. 2017, arXiv:1706.03182 [cs.CV]
[123] Al Musa T, Uddin A, Swoboda PP, Garg P, Fairbairn TA, Dobson LE, et al. Myocardial strain and symptom severity in severe aortic stenosis: insights from cardiovascular magnetic resonance. Quant Imaging Med Surg 2017;7:38–47.
[124] Watson SR, Dormer JD, Fei B. Imaging technologies for cardiac fiber and heart failure: a review. Heart Fail Rev 2018;23:273–89.
[125] Wu MT, Tseng WY, Su MY, Liu CP, Chiou KR, Wedeen VJ, et al. Diffusion tensor magnetic resonance imaging mapping the fiber architecture remodeling in human myocardium after infarction: correlation with viability and wall motion. Circulation 2006;5(114):1036–45.
[126] von Deuster C, Sammut E, Asner L, Nordsletten D, Lamata P, Stoeck CT, et al. Studying dynamic myofiber aggregate reorientation in dilated cardiomyopathy using In vivo magnetic resonance diffusion tensor imaging. Circ Cardiovasc Imaging 2016:9.
[127] Praet J, Manyakov NV, Muchene L, Mai Z, Terzopoulos V, de Backer S, et al. Diffusion kurtosis imaging allows the early detection and longitudinal follow-up of amyloid-β-induced pathology. Alzheimers Res Ther 2018;10:1.
[128] Rabin JS, Perea RD, Buckley RF, Neal TE, Buckner RL, Johnson KA, et al. Global white matter diffusion characteristics predict longitudinal cognitive change independently of amyloid status in clinically normal older adults. Cereb Cortex 2018 [Epub ahead of print]. doi:10.1093/cercor/bhy031.
[129] Amlien IK, Fjell AM. Diffusion tensor imaging of white matter degeneration in Alzheimer's disease and mild cognitive impairment. Neuroscience 2014;276:206–15.
[130] Goergen CJ, Chen HH, Sakadžić S, Srinivasan VJ, Sosnovik DE. Microstructural characterization of myocardial infarction with optical coherence tractography and two-photon microscopy. Physiol Rep 2016;4:e12894.
[131] Mekkaoui C, Reese TG, Jackowski MP, Cauley SF, Setsompop K, Bhat H, et al. Diffusion tractography of the entire left ventricle by using free-breathing accelerated simultaneous multisection imaging. Radiology 2017;282:850–6.
[132] Stoeck CT, von Deuster C, Genet M, Atkinson D, Kozerke S. Second-order motioncompensated spin echo diffusion tensor imaging of the human heart. Magn Reson Med 2016;75:1669–76.
[133] Trifilo MJ, Yajima T, Gu Y, Dalton N, Peterson KL, Race RE, et al. Prion-induced amyloid heart disease with high blood infectivity in transgenic mice. Science 2006;313:94–7.
[134] Ward JE, Ren R, Toraldo G, Soohoo P, Guan J, O'Hara C, et al. Doxycycline reduces fibril formation in a transgenic mouse model of AL amyloidosis. Blood 2011;118:6610–17.
[135] Ueda M, Ageyama N, Nakamura S, Nakamura M, Chambers JK, Misumi Y, et al. Aged vervet monkeys developing transthyretin amyloidosis with the human disease-causing Ile122 allele: a valid pathological model of the human disease. Lab Invest 2012;92:474–84.
[136] Qian J, Huo J, Qian J, Gao T, Gou Y. Novel potential therapeutic strategies of senile cardiac amyloidosis: heat shock factor 1 blocks senile cardiac amyloidosis via HSPA1A in mouse model. Int J Cardiol 2015;195:285–7.